Himalayan Geology, Vol. 26 (1), 2005, pp. 1-18, Printed in India

Himalayan collision zone: new perspectives - its tectonic evolution in a combined ductile shear zone and channel flow model

A. K. JAIN[1], R. M. MANICKAVASAGAM[2], SANDEEP SINGH[1] & S. MUKHERJEE[1]

[1]*Department of Earth Sciences*
[2]*Institute Instrumentation Centre*
Indian Institute of Technology Roorkee, Roorkee-247667

Abstract: The Himalayan Metamorphic Belt (HMB) has been visualized to evolve in a 15–20 km thick Higher Himalayan orogenic channel with the Main Central Thrust (MCT) as one of the boundary wall at its base, and the contact between the Himalayan Detachment Zone (HDZ) and the Tethyan Sedimentary Zone (TSZ) as the other wall. It has undergone 2–stage E = E1 + E2 processes of deformation and exhumation in combined ductile shear and channel flow mode. Initially, most significant pervasive ductile shearing during E1 creates ductile shear fabric with an overthrust top – southwest sense of displacement along direction of tectonic transport, which is indicated by down–dip plunging lineation throughout and across the shear zone as the most pervasive fabric. This creates syn–to post–metamorphic inversion in middle to near–upper parts of the channel, where highest metamorphic grades are disposed of along with the presence of the lower grade rocks in the basal parts of the channel.

During superposed E2 phase, decompression–controlled laminar flow of rock material throughout the channel joins the ongoing top–SW shearing and yields a zone within the channel at the top having an apparent top–NE extensional shearing. U-Pb SHRIMP zircon dates from metasediments, migmatite, biotite granite and in situ leucogranite melt from middle of the Higher Himalayan Crystalline (HHC) reveal that this phase is characterized by extensive migmatization, in-situ episodic granite generation between 46 Ma and 20 Ma in association with ensuing decompression. Granitic melts remain trapped within slab–like core of the channel till these are suddenly released from the chamber around 25–20 Ma, and emplaced near upper channel wall due to rheological variations with the overlying Tethyan sedimentary cover.

INTRODUCTION

Intracontinental continental collision between India and Eurasia since ~ 55 Ma has deformed and remobilized the Proterozoic Indian crust, that is dismembered by numerous thrusts of regional dimensions like the Main Central Thrust (MCT), Vaikrita Thrust (VT), Main Boundary Thrust (MBT) and Main Frontal Thrust (MFT) (Valdiya 1980, Thakur 1993, Srikantia & Bhargava 1998, Hodges 2000, Jain *et al.* 2002) This crust presently occurs as an extensive Himalayan Metamorphic Belt (HMB) throughout its length and has resulted by an initial continental subduction to produce ultrahigh pressure Tso Morari Crystalline (TMC) Belt in the northeast, the Higher Himalayan Crystallines (HHC) and its Tethyan cover in the middle and the Jutogh nappe in the south within a ductile shear zone – the Higher Himalayan Shear Zone (Jain & Anand 1988, Jain & Manickavasagam 1993).

Recent tectonic models regarding evolution of this belt have visualized its evolution mainly in one of the settings: (i) an intracontinental ductile shear zone of regional dimension (Jain & Manickavasagam 1993) and (ii) an extruding channel flow (Nelson *et al.* 1996, Grujic *et al.* 1996). The latter tectonic model has originally emanated from extensive geophysical experiments under the INDEPTH II Project in southern Tibet where partially molten mid-crustal layer is characterized by the following (Nelson *et al.* 1996): (i) P–to–S wave conversion in common – midpoint reflection profiles (CMP) suggesting occurrence of fluids along reflecting horizon, (ii) presence of bright spots of locally anomalous amplitudes in seismic reflections indicating granitic magmas due to partial melting of tectonically thickened crust, (iii) low average S-wave velocity zone in the crust indicating partial melt zone, and (iv) midcrustal resistivites of about 1 to 10 m and extremely high conductivity representing interconnected fluid phase. Keeping in mind the above characters of the Tibetan crust and presence of the Main Himalayan Thrust along which Indian Plate is currently underthrusting, Nelson *et al.* (1996) have visualized that partial molten middle crust (PMC) is apparently added to trailing (down dip) end of the Higher Himalayan Crystalline thrust sheet (HHC), which is displaced upwards and southwards representing progressively older frozen snapshots of the partial molten midcrustal layer lying at depth. Elaborating these concepts through tectonic modeling,

Beaumont *et al.* (2001, 2004) and Jamieson *et al.* (2004) have opined that characters of the Himalaya – Tibet orogen system can be explained through channel flow in middle and lower crust including ductile extrusion of high grade metamorphic rocks and coeval normal faulting and thrusting, which may be ultimately dynamically linked to effects of surface denudation.

Geological details originating from this concept of channel flow are still scanty, though Grujic *et al.* (1996, 2002) and others have provided insight into different geological aspects to this concept with deformation, metamorphism and emplacement of granite melt. Prior to this concept, Jain & Anand (1988) have visualized extensive deformation of the HHC belt within an intracontinental ductile shear zone with ubiquitous overthrust – type ductile shear fabric, having down – dip plunging stretching lineation. Further, inverted metamorphic sequences have been modeled within this belt due to intensely developed ductile shear fabric (Jain & Manickavasagam 1993).

This paper presents geological, deformational, metamorphic, geochronological and numerical modeling inputs of the Himalayan metamorphic Belt (HMB) from the NW Himalaya and puts forward a combined ductile shear zone and channel flow as a plausible tectonic model for the Cenozoic Himalayan collision zone.

GEOLOGICAL FRAMEWORK

The allochthonous HMB contains the Jutogh Nappe in frontal parts within the Lesser Himalaya, the Higher Himalayan Crystallines (HHC) in root zone of the Higher Himalaya, and the Tso Morari Crystalline (TMC) belt in the north. Typically, NE – dipping Main Central Thrust (MCT) at the base and the Himalayan Detachment Zone (HDZ) near the top, delimits the Himalayan Metamorphic Belt (HMB) (Fig. 1). The HMB is thrust southwestward along the folded Jutogh/Main Central Thrust (MCT) or their splays over the frontal Sub-Himalayan para-autochthonous Proterozoic Lesser Himalayan (LH) Shali – Krol Belt in outer parts (Srikantia & Bhargava 1998) and Garhwal-Berinag Group of sequences in parts beneath the MCT (Valdiya 1980). It is characterized by a basal dismembered middle Proterozoic Nirath – Baragaon mylonite augen gneiss of separate Bajura/Kulu thrust sheet (Frank *et al.* 1977). The metamorphic nappe contains an early Paleozoic Mandi Granite (545±12 Ma) of batholithic dimension from Kaplas – Dalhousie to Kurseog. Numerous metamorphic klippe within the Lesser Himalayan terrain also belong to southern parts of this vast pile like the Salkhala Nappe in Kashmir having Paleo-Mesozoic sedimentary cover, Chamba Nappe having the marine Tethyan sedimentary cover, Chail Nappe in Himachal, Garhwal Nappe having the Banali – Satengal – Lansdowne klippe in Garhwal, Almora – Dudatoli Nappe in Garhwal – Kumaon, and Askote – Baijnath – Nandprayag Klippe (Valdiya 1980). Deep erosion of allochthonous metamorphic nappes has exposed the Lesser Himalaya Proterozoic Belt of quartzite, dolomitic limestone, slate, metavolcanics and granite in the Kulu – Rampur Window along Beas – Sutlej Rivers and Kishtwar Window along Chenab River (Sharma 1977).

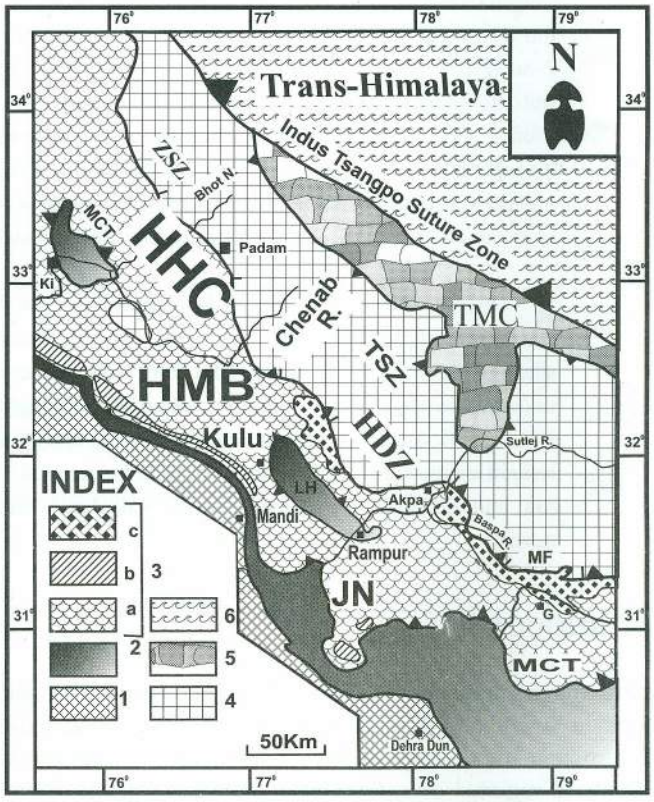

Fig. 1. Simplified geological map of the NW Himalaya. **1**-Sub-Himalayan (SH) Cenozoic foreland basin. **2**-Lesser Himalayan Sedimentary Zone (LHSZ). **3**-Himalayan Metamorphic Belt (HMB): (a) Higher Himalayan Crystalline (HHC) Belt and Jutogh Nappe (JN) with ca. 500 Ma granitoid (b) and Cenozoic leucogranite (c). **4**-Tethyan Sedimentary Zone (TSZ). **5**-Tso Morari Crystalline (TMC) Belt. **6**-Trans-Himalayan tectonic units. Other abbreviations: MBT-Main Boundary Thrust. JT-Jutogh Thrust. MCT- Main Central Thrust. HDZ-Himalayan Detachment Zone including ZSZ-Zanskar Shear Zone and MF- Martoli Fault. ITSZ-Indus Tsangpo Suture Zone (ITSZ). Ki-Kishtwar. S-Shimla. UK-Uttarkashi. G- Gangotri. Compiled from various sources and modified after Jain *et al.* (2003).

The central core of the Himalaya, occupying highest elevation of the Great Himalayan Range, is comprised of the Higher Himalayan Crystalline (HHC) belt of a remobilized basement of about 20 km thick medium to high grade metamorphic sequence. This sequence is intruded by

concordant sheets of Paleo-Proterozoic granitoids in the Munsiari Formation, the Ordovician granitoids of the Pan African event and the Miocene anatectic leucogranite in upper parts. The HHC also incorporates infolded remnants of Paleo – Mesozoic sedimentary sequence in Himachal and Kashmir, but is overlain regionally by the Tethyan Sedimentary Zone (TSZ) along its northern margin as 80 to 100 km wide Paleo-Mesozoic sedimentary cover with a distinct tectonic boundary — Himalayan Detachment Zone (HDZ). In parts of Kashmir, Himachal and Garhwal, this zone has been locally called as the Zanskar Shear Zone (Herren 1987, Patel *et al.* 1993), Rohtang Shear Zone (Jain *et al.* 1999) and Trans-Himadri Thrust (Valdiya 1987) or Martoli Fault, respectively.

Northernmost edge of the HMB is exposed for about 100 km as the Tso-Morari Crystalline (TMC) belt and consists of quartzo – feldspathic gneiss (Puga Formation) and metasediments (Tanglang La Formation), Paleozoic intrusive granitoids (Polokong La granite and Rupshu granite), small thin eclogite and retrogressed amphibolite bodies (Thakur 1993, Girard & Bussy 1999, de Sigoyer *et al.* 2000, Mukherjee & Sachan 2001, Jain *et al.* 2003). This belt is tectonically bound by the Indus Tsangpo Suture Zone (ITSZ) and the TSZ along its entire northeastern and southwestern margins, respectively and evidences of UHP metamorphism at a depth ~ 100 km (Mukherjee & Sachan 2001, Jain *et al.* 2003).

Deformation

Tso Morari Crystalline (TMC)

The Tso Morari Crystalline (TMC) is exposed as a NW – plunging dome on northern slopes of Tanglang La, where thick marble bands and carbonaceous phyllite of the Tanglang La Formation skirt around the fold closure (Fig. 2a). An earliest ductile shear fabric transposes a still older foliation so penetratively that the latter occurs as rootless folds within microlithons only (Fig. 2b). Most of the fabric is asymmetric due to SW-directed overthrust ductile shearing from deep crustal levels and is marked by shear indicators, e.g. asymmetric feldspar augen, pressure fringes, S-C shear fabric, mineral fish etc. and N to NE/S to SW plunging lineation (Fig. 2c). These structures also affect asymmetric eclogite lenses, indicating very strong non – coaxial deformation within the TMC and extensive retrogression of eclogite. All later deformational structures include isoclinal folding of this shear foliation-the D2 deformation that even affects eclogite lenses isoclinally with penetrative axial plane foliation S2. Subsequent NW - plunging open to close folds and their later rotation possibly due to dextral shearing into major structures indicate later deformation. A late stage conjugate extensional foliation dips towards NE and SW irrespective of location of tectonic boundaries of the TMC and represents up-doming effects of leading edge of the Indian Plate under plane strain (Fig. 2d).

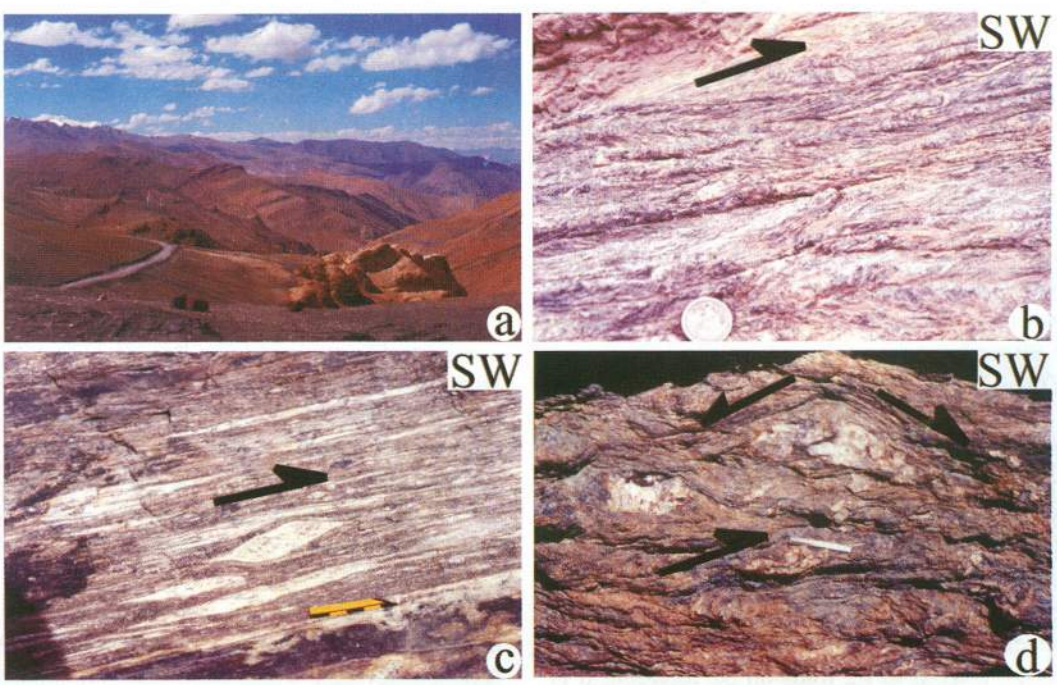

Fig. 2. Structures of the Tso Morari Crystalline (TMC) belt; **(a)** NW-plunging fold closure of the Tso Morari Dome over the Tang La Pass where marble and carbonaceous slate dip both towards SW and NE; **(b)** Rootless relict intrafolial folds bounded by ductile shear zones with top-SW sense of movement within Puga gneiss of the TMC; **(c)** Asymmetrical feldspar megacryst in the Puga gneiss with top-SW sense of movement; and **(d)** Conjugate sets of extensional foliation within the Puga gneiss.

Himalayan Metamorphic Belt (HMB)

The middle part of the HMB, incorporating core of the belt as the Higher Himalayan Crystalline (HHC), has evolved within a major 15 to 20 km thick NE–dipping slab as a result of extreme intracontinental crustal shortening within Indian Plate (Brunel 1986, Mattauer 1986, Jain & Anand 1988). As a consequence, the Main Central Thrust (MCT) and its various splays carry this slab, deformed within the Great Himalayan Channel (earlier recognized as the Higher Himalayan Shear Zone), over the Lesser Himalayan Proterozoic belt (Jain & Anand 1988, Jain & Manickavasagam 1993, 1996, Jain *et al.* 1999, 2003). Our observations from the NW Himalaya indicate that out of four phases of recognizable deformation (D1–D4), D1 deformation has produced isolated, tight and appressed "flame" fold (F1) on lithological banding and/or metamorphic layering (S0). As numerous Proterozoic~1800 – 2000 Ma granitoids are associated with this deformation, it is evident that the HHC incorporates very large component of early Mesoproterozoic metamorphics and relict structures.

Most prominent, intense and widespread Himalayan ductile deformation D2 is characterized by penetrative foliation (S2) paralleling axial surfaces of tight to isoclinal reclined 1C/2 class F2 folds on S0 lithological layering/ metamorphic bandings or earlier S1 foliation. Thinned and boudinaged limbs, thickened hinges and attenuated thickness of F2 folds indicate that P–T conditions were high enough to cause mobilization and flow along quartzo – feldspathic bands during D2 deformation. S2 foliation is essentially a ductile shear composite S-C planar fabric with extreme ductile flow characteristics, regional NW–SE trend and NE dips (Patel *et al.* 1993, Jain & Manickavasagam 1993). S–C shear foliation is invariably associated with asymmetric structures like pressure shadows, augen, sheared lenses, intrafolial folds and rotated porphyroblasts; all structures consistently record top - southwest overthrust ductile shearing throughout the HHC including the upper boundary marked by the Himalayan Detachment Zone (HDZ). Extensive coverage of the HHC throughout the NW Himalaya has demonstrated ubiquitous ductile shearing along S2 foliation that has resulted in transposition and obliteration of all earlier structures and development of most prominent S-C shear fabric, where all earlier foliations/lithological banding behave like S-fabric. As a result, mineral/stretching lineation (L2/Lm), rodding and boudinage, representing the extensive flow direction within the channel/shear zone, are the most prominent linear features, which are coaxial to F2 folds on S2 foliation. It is defined by preferred orientation of many prismatic and tabular minerals including kyanite, staurolite, sillimanite, biotite, muscovite, and acicular prismatic amphibole crystals in lithologies of various metamorphic grades. Within mylonitized and deformed leucogranite, L2 stretching lineation is defined by tourmaline, quartz and feldspar. All these structures regionally trend orthogonal to the Himalayan orogen and appear to have developed during ductile extrusion throughout the Himalaya in direction of tectonic transport representing X-direction of strain ellipsoid during top-southwest ductile shearing (also Coward *et al.* 1982, Brunel 1986, Jain & Anand 1988, Epard *et al.* 1995, Grujic *et al.* 2002). L2 plunges consistently 15-40 ^{0} down – dip with very high pitch angle on S2 foliation. Such a pattern is not only confined to the HHC, but extends to the HDZ, the overlying TSZ cover to the Proterozoic basement, the Vaikrita and Munsiari Thrust zones, and footwall of the Lesser Himalayan Sedimentary Zone (Brunel 1986, Mattatauer 1986, Patel *et al.* 1993, Jain & Patel 1999, Jain *et al.* 1999).

Compressional D3 deformational phase is superposed on all the earlier fabric and subdivided into two distinct episodes. Early D3a deformation is represented by close to isoclinal recumbent to gently inclined 1B/1C3 F3a folds on earlier composite S1S2 and/or C-foliation, axial plane foliation (S3a) and L3a mineral lineation. F3a folds are developed on all scales including most spectacular large folds in Zanskar and Himachal Pradesh. F3a folds resulting type-2 interference patterns obliquely refold S2 axial plane foliation and limbs of F2 folds. S3a axial plane foliation of these folds is defined by alternating quartzofeldspar and muscovitebiotite-rich layers, cutting across the folded S2 foliation in hinge zones of F3a folds with moderate dips towards NE or SW. Biotite-muscovite flakes, sillimanite and kyanite define a faint mineral lineation (L3a, which parallel F3a fold hinges. Subsequently, open to close (F3b) crenulation folds of class1B type with characteristic crenulation foliation (S3b) are developed on earlier planar fabrics during the D3b deformation. Along hinge zones of the F3b folds, L2 lineation is folded along with S3a axial planes and F3a limbs. These F3b folds are coaxial to F3a folds and result in type3 interference patterns. However, F3b folds producing type2 interference patterns obliquely refold the S2 foliation and F2 limbs. Intersection of crenulation foliation with S1, S2 and S3a surfaces and smallscale F3b crenulation axes define the L3b lineation. In mica-rich rocks, mica flakes parallel to the F3b crenulation folds characterize L3b lineation.

At a number of places within the HMB, discrete and intensely sheared gently dipping zones have fault gouge of fragmented rocks, which post -date S3b crenulation foliation and appear to represent late phase of brittle thrusting due to the MCT. Kink bands, tension gashes, slickensides and joints are developed on earlier foliations during D4 deformation.

One of the important event of the D4 event is the presence of large-scale open and upright cross-folds that produce culminations and depressions, and control outcrop patterns of many structures. These trend almost orthogonal to the arcuate Himalayan trend, whose axial surfaces trend NE-SW, N-S and NNW-SSE from western parts towards east and represent post-main thrusting events.

Distinct extensional structures on earlier foliation planes are formed during progressive deformation including extensional crenulation cleavage/foliation (ecc) and foliation boudinage. It has produced extension parallel to the single set or conjugate sets, thus causing shear sense reversal within the HDZ and elsewhere. Within many thrust zones and also within the HMB, single and conjugate extension crenulation foliation (ecc) provide undisputed evidences of extension parallel to the pre-existing foliation and shortening normal to foliation planes. In foliated rocks, two extensional crenulation foliation sets may even produce foliation boudinage.

Himalayan Detachment Zone (HDZ)

Northernmost and uppermost boundary of the HHC has now been identified as a complex tectonic zone, having an initial top-SW overthrust movement, observed rarely in the northwestern parts, followed by top-NE extensional faulting almost throughout the Himalaya from Zanskar to Nepal. Burchfiel *et al.* (1992) have designated this boundary as the South Tibetan Detachment System (STDS); others have called it as the Trans-Himadri Thrust/Fault (Valdiya 1987, 1989). In this work, it has been regionally redesignated as the Himalayan Detachment Zone (HDZ). This shear zone has been mapped for almost 1700 km now from Suru Valley in Zanskar to northernmost parts of Sikkim. It has been identified as the Zanskar Shear Zone (ZSZ) in southern Ladakh (Herren 1987, Patel *et al.* 1993), Rohtang Shear Zone (RSZ) in the Beas Valley, Himachal Pradesh (Jain *et al.* 1999), Jhala Normal Fault in the Bhagirathi Valley, Garhwal (Metcalfe 1993), Malari Fault/Martoli Fault/Dar-Martoli Fault in parts of upper Bhagirathi, Dhauli–Gori–Kali Valleys, Annapurna fault/detachment and South Tibetan Detachment System (STDS) by Pêcher *et al.* (1991), Burchfiel & Royden (1985), Burchfiel *et al.* (1992) and Searle & Godin (2003).

Zanskar Shear Zone (ZSZ)

As a part of the HDZ, one of the best known NW-SE trending Zanskar Shear Zone defines northern margin of the HHC in parts of the Suru-Doda Valleys, Zanskar (Herren 1987, Patel *et al.* 1993) within overall main compressional tectonics. Herren (1987) has identified prominent extensional shear zone of 2.25 to 6.7 km width, which is marked by intense mylonitization, asymmetric shear indicators like S-C planes, mineral augen, boundins, pressure shadows, grain-shape fabric and broken fragments. Metamorphic isograds are telescoped within upper greenschist and lower amphibolite facies, having minimum horizontal displacement of 16 km with a vertical component of 19 km. Detailed structural observations along almost entire length of the ZSZ, however, reveal that it is characterized by an earlier top –SW sense of overthrust ductile shearing (Fig. 3a), which is superposed by NE-SW oriented extension along the ZSZ (Patel *et al.* 1993), thus causing shear sense reversal within the shear zone (Fig. 3b). It is also noteworthy that such a shear zone occurs within an overall domain of overthrust geometry where the Paleozoic Tethyan sedimentary sequences are imbricated by numerous thrusts and overridden by younger formations in the north (Baud *et al.* 1984, Patel *et al.* 1993). The presence of augen mylonitic xenoliths within deformed tourmaline leucogranite tabular sheet (~22 Ma) along a shear zone supports an earlier ductile top-SW shearing along the ZSZ prior to leucogranite emplacement (Fig. 3c). The ZSZ is marked by ductile structures and textures affecting high-grade staurolite-kyanite and sillimanite-muscovite grade rocks at deeper crustal levels. However, brittle-ductile and brittle shear zones also demarcate this boundary. In contrast to the observations by Herren (1987), consistent reclined folds plunge almost uniformly towards NE with an axial plane foliation S2 and a very prominent stretching down – dip plunging lineation, not only within the shear zone but also away within the HHC. Numerous shear criteria reveal a ubiquitous top – southwest overthrust sense of ductile shearing (Patel *et al.* 1993), superposed extensional crenulation foliations indicating layer-parallel extension. Many of these are occupied by melt-enhanced leucogranite veinlets indicating close relationship between extensional tectonics, exhumation and decompression melting (Fig. 3d).

In southeast along the ZSZ, upper parts of the HHC sequence is characterized by gently to moderately dipping migmatite and anatectic leucosomes in lower parts, an intrusion complex of dense leucogranite dykes and sheet like – pluton and about 1 km thick pelitic mylonitic zone in kyanite to biotite zone (Dezes *et al.* 1999). Dezes *et al.* (1999) critically observed, like Patel *et al.* (1993), that extension along the ZSZ is superposed on the southwest verging imbricate major synmetamorphic thrust along the HHC and TSZ boundary. A continuous metamorphic sequence, marked by kyanite to biotite isograds in P-T range of 550 to 700^{0}C and 5.9 to 9.1 KB, is preserved within the shear zone. Assuming present-day dip of 20^0, a net displacement of 35±9 km has been calculated

with a minimum estimate of vertical movement of ~12±3 km through ductile simple shear by them. U-Pb monazite ages constrain cooling of leucogranite around 22.0±0.2 and 22.5±1 Ma in the ZSZ and compares well with timing of crustal anatexis and leucogranite intrusion in Zanskar between 22 and 19 Ma (Noble & Searle 1995).

Further extension of the HDZ is seen along the Beas Valley on high slopes of the Rohtang Pass where the Rohtang Shear Zone delineates the gneiss from the low grade Haimanta Formation (Jain *et al.* 1999). Along the Sutlej Valley, two distinct detachment zones characterize the HHC at Karcham and Akpa; both are marked by intense migmatization of high-grade metamorphics and partial melting with leucogranite generation and presence of Himalayan granite at Akpa. These zones are marked by top-SW overthrust and top-NE extensional movements during ductile shearing which has produced trains of intrafolial folds within narrow shear zones whose boundaries are presently occupied by leucogranite (Figs. 4a, b).

HIMALAYAN METAMORPHISM

Tso Morari Crystallines (TMC)

As the northernmost part of the HMB, the Tso Morari Crystalline (TMC) dome consists of gneissic Puga Formation of Cambro-Ordovician age, overlying Paleo-Mesozoic psammite, pelite, metamarl, marble and metabasalt as well as Paleozoic granitoids. Metabasics occur as eclogite lenses and have undergone amphibolite to greenschist facies retrogression with relict eclogitic cores, which are marginally sheared and boundinaged.

Eclogite contains garnet, phengite, clinopyroxene, omphacite, carbonates, rutile and rarely plagioclase with decreasing abundance. Retrogressed eclogite lenses contain amphibole, paragonite, quartz, biotite, epidote and zoisite (Guillot *et al.* 1997). Main matrix contains amphibole, phengite and quartz containing idioblastic to sub-idioblastic garnet and omphacite. Garnet is mostly grossular-rich with

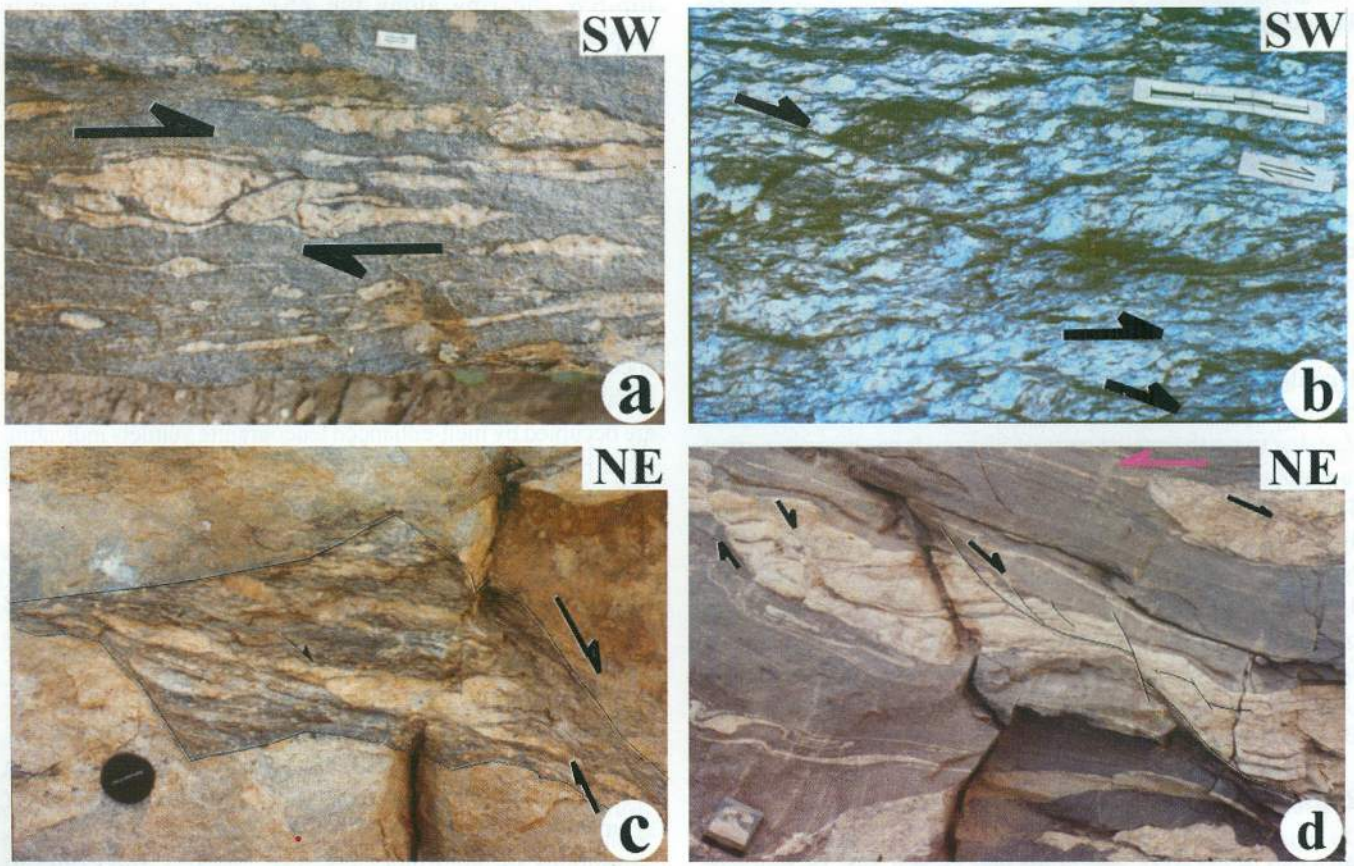

Fig. 3. Structures from the Himalayan Detachment Zone (HDZ). **(a)** Zanskar Shear Zone with mylonitized migmatitic gneiss with feldspar megacryst showing top-SW sense of movement; **(b)** Megacrystic mylonitized granite gneiss from the ZSZ with top-NE ductile shearing; **(c)** Mylonite enclave within the Himalayan leucogranite indicating main movements along the ZSZ pre-dating the leucogranite emplacement; and **(d)** Migmatitic gneiss of the HHC within the ZSZ having extensional foliation.

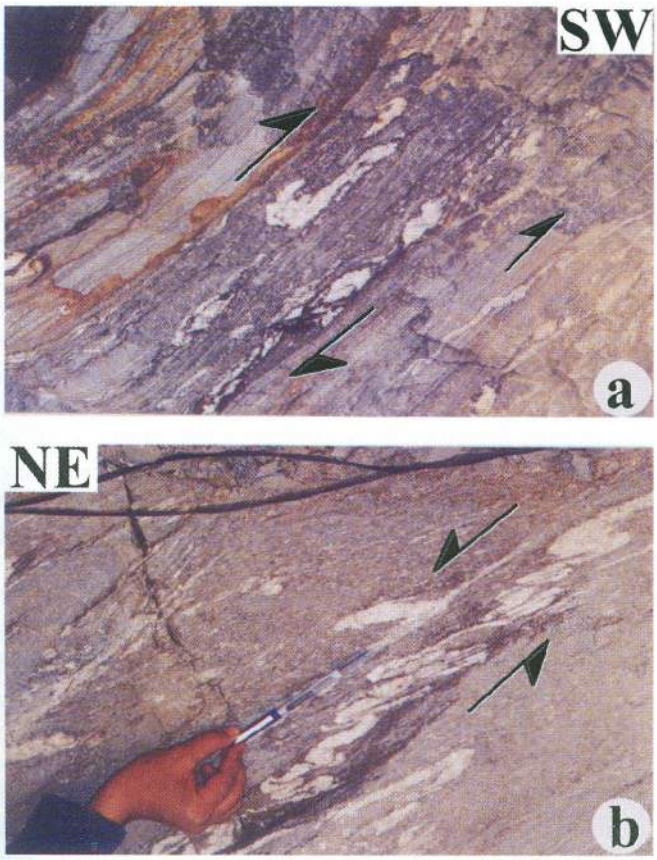

Fig. 4. Structures of the Himalayan Detachment Zone (HDZ) along the Sutlej Valley. **(a)** Rootless intrafolial folds within overthrust shear zone of migmatite showing top-SW shear sense and **(b)** Nearby outcrop showing top-NE and downward sense of ductile shearing. Note leucogranite veinlets occupying extensional shear zone as in situ produced melts.

occasional zoned pyrope-rich almandine varieties. Garnet cores have inclusions of orthopyroxene, clinopyroxene, rutile, amphibole, mica and quartz, and only rutile along the rim. Garnet is cracked radially around coesite inclusions (Mukherjee & Sachan 2001). Omphacite has quartz, rutile and zircon inclusions. Amphibole of varying composition is predominant in matrix having quartz and rutile inclusions and shows compositional zoning. Omphacite has >0.7% Na and about 1.00 to 2.00 % Na in retrogressed varieties.

P-T estimates for eclogite, mica schist and amphibolite using conventional multiple thermobarometric and thermocalc methods on garnet rims with coexisting equilibrium minerals give ~850°C using garnet-clinopyroxene and garnet-muscovite (phengite) thermometers and 28.9 Kb from garnet-clinopyroxene-phengite barometer. P-T data, estimated by thermocalc method for the same assemblages, give 856± 83°C and 26.4±2.8 Kb. Garnet core temperatures with amphibole and phengite inclusions yield 630 to 700°C. Increase in temperature from core to rim is evident from prograde growth zoning in garnet. In retrogressed eclogite, conventional methods could only be used due to incomplete reactions and give 500–600°C and 8.5 to 13.0 Kb. Re-calculated rim–matrix and core–inclusions compositional data of Guillot *et al.* (1997) yield 680±57°C/ 19.0±2.4 Kb and 700±73°C/22.7±2.7 Kb by thermocalc method, and 480–650°C/ 16.0-19 Kb and 650-690°C/28.8-30 Kb by conventional method. Similarly, re-calculated rim data of Mukherjee & Sachan (2001) gave 712±95°C/33.4±4.1 Kb by thermocalc method, and 470-750°C/27.0 - 28 Kb by conventional method.

P-T data of Tso Morari eclogite suggest that these have formed at peak temperatures and pressures ~750 to 850°C and 27 to 29 Kb (cf. O'Brien *et al.* 2001). Guillot *et al.* (1997) have worked out second and third metamorphic stages on the basis of stability of glaucophane, clinopyroxene-plagioclase symplectite and ferroparagsite-edenite transformations with reduction in pressures of 11.0 to 8.0 Kb with a temperature increase of ~30 to 40°C in third stage, which indicates heating during decompression with concomitant retrogression. Our data show similar results for most of the samples with re-equilibrated amphibole-rich assemblage. This suggests reduced P–T conditions from peak metamorphism with no heating during later re-equilibration and exhumation, as is also evident from associated mica gneiss showing ~ 650°C and ~16 Kb. This implies that the TMC eclogites have undergone medium temperature and high-pressure peak metamorphism during continental subduction of the Indian plate along the ITSZ.

Higher Himalayan Crystalline

The HMB incorporates pelite, psammite and quartzite together with thin amphibolite and calc-silicate bands and different varieties of Proterozoic and Paleozoic granitoids, which are extensively deformed and metamorphosed under middle green schist to almandine-amphibolite facies (Pognante *et al.* 1990, Epard *etal.* 1995, Noble & Searle 1995, Jain *et al.* 1999, Manickavasagam *et al.* 1999, Vance & Harris 1999, Stephenson *et al.* 2000). Three metamorphic episodes, i.e. pre-Himalayan (M1), main Himalayan (M2) and post-Himalayan (post-M2), have been identified in the HMB. The earliest M1 metamorphism, (cf. Manickavasagam *et al.* 1999) has largely been superposed and obliterated by later main Himalayan M2 metamorphism from base to the top during intense penetrative D2 deformation and is evident from syntectonic garnet, hornblende, staurolite and kyanite porphyroblastic growth, development of asymmetric quartz/ feldspar augen and pressure shadows along both S-and C-

surfaces. Garnet porphyroblast shows rotated inclusions with overgrown subidioblastic inclusion-free late-to post-tectonic rim, which grew during late-to post-D2 deformation and M2 metamorphism. Mineral lineation L2 on main foliation is indicated by preferred orientation like mica, kyanite, sillimanite, hornblende etc. during this metamorphism. However, Hodges and Silverberg (1988) and Pognante *et al.* (1990) have called this metamorphic episode as M1 Barrovian metamorphism (Eohimalayan) in the lower parts reaching up to kyanite grade and M2 sillimanite grade metamorphism (Neohimalayan) with migmatite and leucogranite generation in middle and higher structural levels during movements along the MCT and ZSZ in later period. Post-M2 metamorphism is manifested by quartz, muscovite and biotite growth along S3 foliation in hinge zones and axial traces of the F3 folds.

In Zanskar, base of the HHC adjacent to the MCT is marked by staurolite – kyanite grade, where garnet core and rim record temperature and pressure of 500-550°C/8 Kb and 600-650°C/8-9 KB, respectively. Core temperature increases in the upper structural levels and reaches a maximum of 780°C in sillimanite-K-feldspar grade, but with no significant change in core pressure. The HHC in higher grades reveal reduced rim temperature of 600 to 650°C from that of the core and similar temperature in the basal parts. However, garnet rim have shown significant pressure reduction to 4-6 KB in the highest grade. Temperature increase in basal parts has been associated to faster exhumation of higher metamorphic grades relative to the basal part in association with the thermal relaxation, re-equilibration and heating of basal part prior to movements along the MCT. However, based on garnet core and rim data, Stephenson *et al.* (2000) have suggested that there is an inversion in the MCT zone with an increase in temperature to a maximum of 742±53°C and at constant pressure of 9.6±1.8 Kb for highest grade during M1 metamorphism, prior to localized sillimanite growth during M2 metamorphism. Metamorphic gradients are attributed to polyphase metamorphism and post-metamorphic ductile thrusting. It has been suggested that lower MCT zone preserves peak M2 metamorphic condition and is juxtaposed by upper MCT and HHC units, which have preserved retrograded equilibrium conditions, and are superposed upon lower MCT during post – M2 metamorphism.

In Sutlej Valley, lower parts of the HHC up to the Vaikrita Thrust indicate garnet to sillimanite zones, whereas staurolite-kyanite, sillimanite-K-feldspar zones are observed from the base to higher structural levels above the Vaikrita Thrust (Manickavasagam *et al.* 1999). Rim thermobarometric results in lower parts of the HHC up to Vaikrita Thrust indicate a uniform temperature of 610±10°C but pressure increases from 6 Kb in garnet zone to 10 Kb in staurolite zone. However, Vannay & Grasemann (1998) have observed similar temperatures but reduction in pressures from 9.5 Kb in garnet zone to 6 Kb in kyanite/sillimanite zone. Above the Vaikrita Thrust, staurolite zone gave similar P–T conditions in lower part, but sillimanite and migmatite zones recorded 740- 800°C and ~9 Kb (Manickavasagam *et al.* 1999). However, Vannay & Grasemann (1998) reported an average temperature of 570±30°C for all the zones above the Vaikrita Thrust with pressure reduction from 7.5 Kb in staurolite to 5 Kb above the Vaikrita Thrust in migmatite zone, suggesting that lower P-T conditions are due to re-equilibration during exhumation and cooling. Oxygen isotope thermometry combined with net transfer reactions for lower part of the HHC below the Vaikrita Thrust recorded temperature from 610-700°C and pressure from 9-7 Kb from base up to the Thrust (Vannay *et al.* 1999). Above this thrust, temperature increased from 570 to 750°C at nearly constant pressure of 8 Kb from base up to migmatite zone at higher structural level.

In Alaknanda and Dhauli Ganga Valleys, Hodges & Silverberg (1988) have suggested two metamorphic episodes where initial M1 Barrovian metamorphism is followed by Buchan M2 metamorphism. The basal part kyanite grade garnet rims of M1 indicated about 570°C and 9.6 Kb, whereas M2 gave about 642°C and 5.2 Kb for the upper part. M1 is attributed to burial to a depth of 36 km during early stages of collision and M2 is related to thrust imbrication during uplift and second burial to a depth of 5 to 7 km with associated heating.

Timing of peak metamorphism in Zanskar region yielded 32 to 30 Ma for monazite (Walker *et al.* 1999) and 33-31 Ma and 31 to 28 Ma for Sm-Nd garnet for the core and rim (Vance & Harris 1999) and suggested that prograde M1 metamorphism took place between 35 and 25 Ma age. Migmatite and leucogranite yielded 20.6 to 19.5 Ma and 20.8±0.3 Ma (Noble & Searle 1995) and these ages have been attributed to M2 sillimanite grade metamorphism and crustal melting.

Inverted Metamorphism

Inverted metamorphism in the NW Himalaya is common across the HHC within the MCT zone, and also in the LH nappes. It is either continuous in sections like Zanskar or affected by intervening thrusts in other sections of Sutlej and Bhagirathi Valleys. Hodges & Silverberg (1988) and Hubbard (1989) are of the opinion that this inverted metamorphism is apparent, while others have considered it as real (Le Fort 1975, Pêcher 1989, Jain & Manickavasagam 1993, 1997). Various models have been proposed for this phenomenon

and include (i) hot-over-cold model due to crystalline belt, (ii) frictional shear heating due to thrusting along the MCT, (iii) leucogranite emplacement at higher levels, (iv) recumbent folding and thrust imbrication, and (v) ductile shearing within intracontinental shear zone.

On the basis of textural, mineral growth and thermobarometric data from SE Kashmir and limitations of previous models, Jain & Manickavasagam (1993, also, Jain & Manickavasagam 1996, Jain *et al.* 1999, Manickavasagam *et al.* 1999) have proposed that prograde regional metamorphic isograds within the HHC got inverted in a ductile shear zone due to S-C ductile shear fabric. Prograde regional metamorphism was attained up to a maximum depth of 25-35 km, possibly during continental subduction of the Indian Plate when this belt attained temperature and pressure of 550 to 780°C and 5 to 11 Kb. Garnet, staurolite, kyanite and sillimanite grew along main foliation during D2 deformation event and superposed C-foliation in a non-coaxial intracontinental ductile shear zone. During this process, millimetre–spaced C–foliation sigmoidally bent the S-foliations on small-scale towards southwest in the direction of ductile tectonic transport (Jain & Manickavasagam 1993). This model postulates that isograd boundaries also underwent small-scale displacements along C-foliation in the ductile shear zone with a cumulative minimum displacement ~80120 km within a 20 km thick ductile shear zone (Fig. 5). Present-day distribution of individual isograd boundaries in different parts of the NW Himalaya is largely controlled by interaction of various factors, such as (i) dip of the ductile shear zone, (ii) displacement within subsidiary and locally-developed ductile zones due high shear strain, (iii) interaction between exhumation and ductile shearing, (iv) later superposed folds, (v) level of present-day erosion, and lastly (vii) mutual relationship between large dislocations/thrust and isograd boundaries.

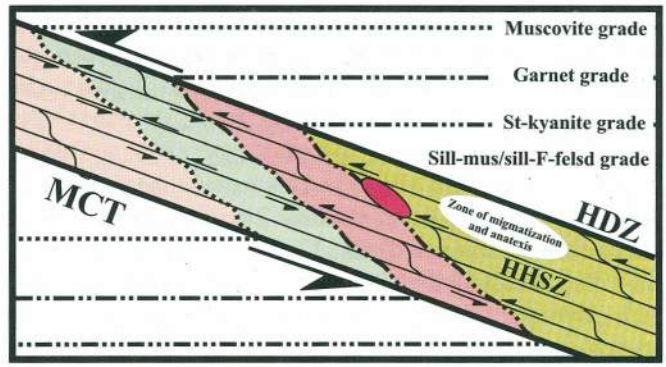

Fig. 5. Tectonic model for Himalayan inverted metamorphism. Ductile shear zone model showing penetrative ductile shearing and S-C shear fabric (curved lines) as a cause of inverting metamorphic isograds within intracontinental shear zone. Zone of anataxis and in situ leucogranite are associated with migmatite and decompressional melting during exhumation in sillimanite-muscovite isograd/sillimanite-K-feldspar isograd (triple dots). Other isograd boundaries are indicated by single dots-garnet isograd and double dots-staurolite-kyanite isograd. Small arrows show movement sense within Higher Himalayan Shear Zone (HHSZ) bounded by the Main Central Thrust (MCT) at the base and Himalayan Detachment Zone (HDZ) at the top.

SHRIMP U-Pb Zircon Dating

One of the many characteristic features of the Himalayan orogenic belt is the generation and emplacement of the Miocene leucogranite during a very short span between 24 and 19 Ma along northern margin of the HHC (Davidson *et al.* 1997, Harrison *et al.* 1997, 1999, Searle *et al.* 2003). Their crystallization ages are much younger than peak Himalayan metamorphism in Zanskar (37-28 Ma - Vance & Harris 1999, Walker *et al.* 1999) and Garhwal (44-26 Ma –Foster *et al.* 2000, Prince *et al.* 2000, 2001). Gap between Eocene-Oligocene Himalayan metamorphism and subsequent generation of Miocene leucogranite has been explained either by thickening of Indian Plate (Treloar *et al.* 1989, Pognante *et al.* 1993) or by slab break off (Guillot *et al.* 1997).

In the northwest along major sections like Zanskar, Sutlej, Beas, Bhagirathi and Alaknanda Valleys, leucogranite belt is widely developed almost at the top of the HHC beneath Tethyan sequence with very sharp contacts for many kilometers away from narrow migmatite zone, having extreme flowage within high-grade metamorphics. Sillimanite– kyanite – mica schist/gneiss passes gradually into migmatite with development of leucogranite veinlets along main foliation (Fig. 6a). Various shear indicators like σ–shaped asymmetrical augen, SC shear fabric and associated gneiss reveal consistent top–SW verging overthrust tectonic movements within migmatite (Fig. 6b). Discrete ductile thrusts are superposed upon penetrative shear fabric and may represent later episodic overthrust events. Extensional crenulation foliation, shear bands and foliation boudinage reveals extension within migmatite (Fig. 6c). Of interest is the presence of conjugate set of cross-cutting extensional foliation whose planes are characterized by discrete and noteworthy melt-enhanced deformation (Fig. 6d). P-T calculations by garnet-biotite-muscovite– plagioclase-sillimanite/kyanite-quartz assemblage yield 757±8°C for garnet core and 700±10°C and 8.9 to 10.7 Kb for garnet rim in sillimanite–muscovite grade metamorphism in the Bhagirathi Valley (Manickavasagam *et al.* 1999, Jain *et al.* 2002), though distinct decompression patterns are discernible from Zanskar with reduction in garnet rim pressure to 4-6 Kb (Jain & Manickavasagam 1993).

As a possible source of leucogranite from migmatite, cathodoluminescence (CL) imaging and U-Pb SHRIMP dating of zircons from sillimanite-muscovite schist/gneiss,

migmatite, biotite granite and *in situ* tourmaline–bearing leucogranite (TBL) from the Bhagirathi-Valley near Lohari Nag have been carried out. Polished mounts of hand – picked zircon separates along with CZ3 Sri Lankan zircon standard ($^{206}Pb/^{238}U$ = 0.0914 and age of 564 Ma) were examined under backscattered electron (BSE) and cathodoluminescence (CL) imagery using a JEOL 6400 SEM. Zircons separates are of varied shapes from a few tens of μm to ~400 μm. CL images show that almost all the grains have somewhat rounded cores with three distinct zones - an inner core, a spongy middle portion and clear rim (Fig. 7). Data from rim analyses reveal Th/U ratios <0.1 and zircon overgrowths range between 46 and 20 Ma with an episodic pattern. These ages indicate that zircon growth persisted over protracted time span during M2 metamorphism of the HHC. Decompression and exhumation leads to squeezing of melt from rocks along shear fabric, which may have been accentuated by the presence of melt.

Episodic zircon growth from 46 to 20 Ma reveal syntectonic character of migmatite when the melt was generated in overthickend crust since ~45 Ma. Formation of this hot, low-viscous, mid-crustal migmatite leads to the initiation of channel causing outward flow of material. This viscosity reduction has resulted from small percentage of partial melt ~700 to 750°C and is further enhanced by metamorphic devolatilizing reactions. This outflow material is the first evidence of initiation of magmatic fluids in the Great Himalayan Channel around 45 Ma in association with exhumation – controlled development of migmatite zone.

NUMERICAL MODELING

Exhumation within the Higher Himalayan Shear Zone (HHSZ) in Zanskar is numerically modeled as a two-stage process: (i) E1-crustal shortening due to top-SW relative sense of movement between the Main Central Thrust (MCT) and top of the Zanskar Shear Zone (ZSZ) during early phase, which deforms whole of the HHC southwestwards by numerous ductile shear zones, (ii) E2-extensional shearing along the ZSZ, concomitantly to the ongoing thrusting along the MCT during Early Miocene that resulted in fast exhumation of the HHC along the same shear planes produced during the E1.

Existing models of the HHC exhumation (see Hodges 2000 for review) are studied and none of them are found to give a complete picture of E = E1 + E2. For example, Ductile

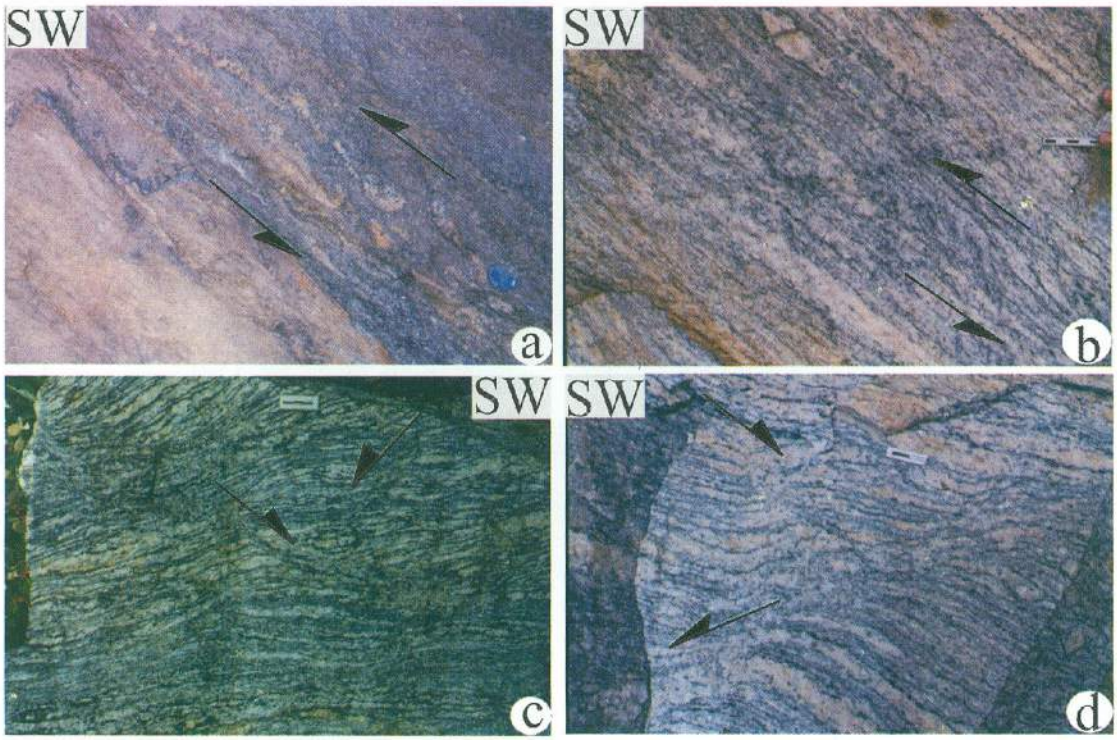

Fig. 6. Migmatite from the HHC and its structures. **(a)** Himalayan changing into migmatite with introduction of concordant leucosomes along main S2 foliation near Lohari Nag along Bhagirathi Valley, **(b)** Top-SW ductile shearing within migmatite having asymmetrical feldspar megacryst and S-C shear fabric at the same locality, **(c)** Conjugate set of extensional foliation with granite melt in migmatite near Sumcham along the Bhot Nadi- a tributary of Chenab River in Padar, Jammu and Kashmir, and **(d)** Melt-enhanced deformation features along extensional shear zone from the Bhagirathi Valley near Lohari Nag showing foliation with top –downward movement.

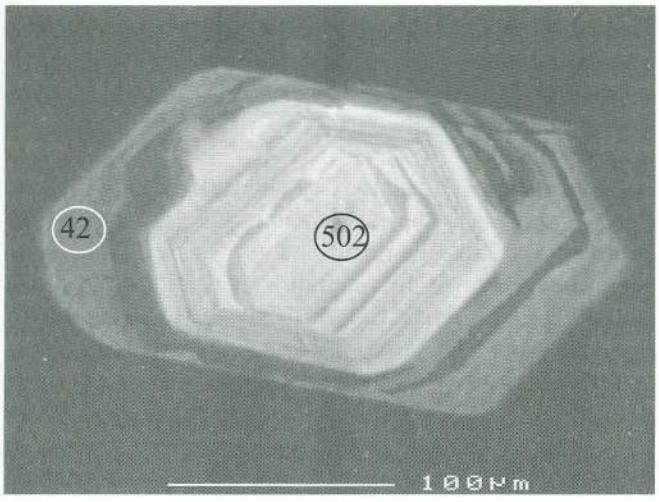

Fig. 7. CL image of zircon from migmatite of the HHC from the Bhagirathi Valley.

Shear Model, originally proposed by Jain & Manickavasagam (1993) for the HHSZ, provides insight only to the E1 phase. On the other hand, Channel Flow Model (Grujic *et al.* 1996) for the exhumation of the HHC in Bhutan takes care only the top-NE sense of shearing within the South Tibetan Detachment System or in its different counterparts (e.g., Dèzes *et al.* 1999), while ubiquitous early top-SW sense of shear within the Zanskar Shear Zone (Patel *et al.* 1993, Dèzes *et al.* 1999) remains unexplained. Keeping these difficulties in mind, a combined model for exhumation E is presented. With unavailability of actual rock flow equations, fluid mechanics approach has been introduced as a first approximation to represent rock flow. All the flows have been considered laminar since rate of deformation is essentially very slow and not turbulent in geological condition for ductile deformation.

E1 Phase

Considering the MCT and the top of the ZSZ as two walls of the HHSZ like an orogenic channel, E1 is given by shear flow of the HHC that is completely controlled by shearing between the channel walls (ductile shear flow). E2 is approximated by a combination of the Poiseuille flow (flow induced solely by pressure gradient) and the earlier flow type.

E1 phase can be represented by non-coaxial ductile shearing of a marker line AB, initially perpendicular to the parallel-walled channel X and Y (infinitely long) and filled in with incompressible fluid with a viscosity μ, governed solely by wall velocities U_X and U_Y respectively, one in opposite direction to the other with choice of axes and symbols as in Figure 8a, velocity profile is given by:

$$x = (U_X - U_Y)/2 + \{(U_X + U_Y)/2\ y_0\}\ y,$$

which is also the mathematical representation of Jain & Manickavasagam's (1993) 'Ductile Shear Model'. The pivot (P) coordinate about which AB rotates is given by $[0, y_0 (U_Y - U_X)/(U_X + U_Y)]$, which means that position of P is determined by wall velocities and thickness of the channel. Geological significance of P is that, except for a horizontal channel, and U_X, U_Y not equal to zero, exhumation and subduction will be simultaneous processes: if the BP part of the channel undergoes exhumation, AP will undergo subduction and vice versa. For a non-horizontal channel, if either U_X or $U_Y = 0$, the whole process would either be only subduction or only exhumation. It is postulated that metamorphic isograds within the Higher Himalaya were kinked during E1, and made acute angle with top of the ZSZ in the top – NE direction (and were subsequently modified in the next exhumation phase). Although the term ZSZ has been used in this phase, it didn't have a separate entity during E1. Fig. 8b represents the S-C shear fabric orientation at this stage within the Higher Himalaya as an example of the shear sense indicator and is supported by the fact of its ubiquitous distribution throughout the HHC including the ZSZ (Patel *et al.* 1993, Dèzes *et al.* 1999), and even in the Tethyan Sedimentary Zone at its top.

E2 Phase

The E2 exhumation phase is given in Figure 8c, where the fluid moves both due to channel wall movement as well as the fluid pressure gradient (dP/dx). The velocity profile is given by:

$$x = (U_X - U_Y)/2 + (U_X + U_Y)\ y/2\ y_0 - (1/2\ \mu)\ dP/dx\ (y_0^2 - y^2)$$

A line passing through V/ and parallel to the MCT (Z in our diagram) marks the lower boundary of the ZSZ. Some of the earlier D_2 shear fabrics within the ZSZ were reoriented giving top-to-NE shear sense during this bulk southwestward flow, but some escaped this retro-shear along the same C-plains and remained as remnants (Fig. 8d, e). The angle between the isograds and the top–NE direction at base of the ZSZ decreased further and remained acute, whereas that with the top of the ZSZ was increased, thus making an obtuse angle to the NE direction. E2 phase is also marked by anataxis and migmatization, and subsequent leucogranite injection at the base of the ZSZ. The extensional crenulation cleavage, antithetic to, and cross-cutting the D2 top-SW shear fabric in the ZSZ (Patel *et al.* 1993), may be synchronous with this late top-NE sense of shear phase and may be its secondary synthetic shear planes. Top-SW sense of shear, on the other hand, continued within the HHC during this phase.

DISCUSSION

Recent investigations of the HMB have revealed that northern leading edge of the Indian Plate appears to have subducted

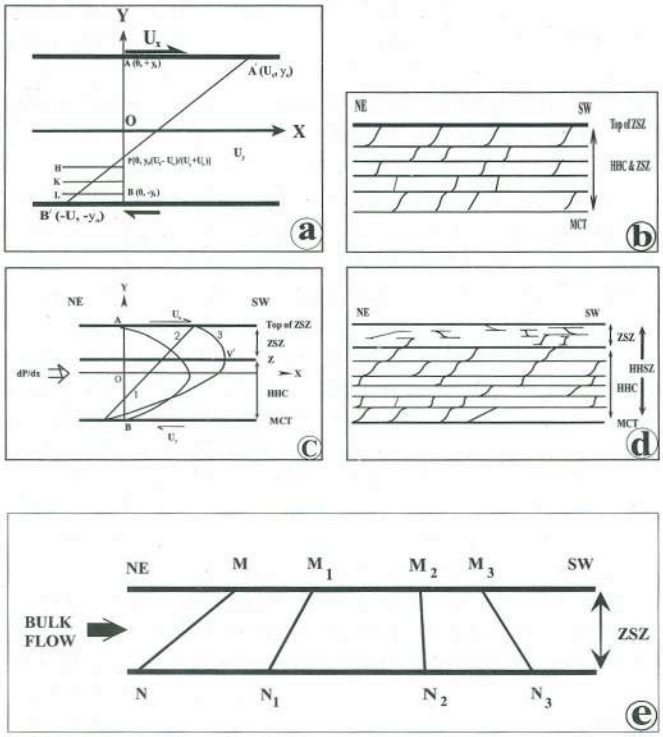

Fig. 8. **(a)** Ductile Shear Model showing non-coaxial deformation of marker AB due to ductile shear on its two channel walls X and Y with velocities U_X and U_Y respectively, one in opposite direction to the other. See text for details, **(b)** Structural significance of ductile shear flow. Althrough the HHC and ZSZ a consistent top–SW shear sense developed within the HHSZ, as deciphered from numerous S–C fabrics. (Not to scale), **(c)** With the same choice of axes as in Fig. 8 (a), marker line 1 represents the velocity profile for ductile shear flow of a marker AB, parabola 2 represents the velocity profile for a Poiseuille flow, and. curve 3 represents the velocity profile for a combined flow when both ductile shear and the Poiseuille flow are active. Thickness of the ZSZ is not to scale. See text for more details, **(d)** Structural significance of such combined flow within the HHSZ. A line parallel to the MCT marks the lower boundary of the ZSZ. Some of the earlier D2 shear fabrics within the ZSZ were reoriented giving top-NE sense during this bulk southwestward flow, but some escaped this retro-shear along the same C-plains and remained as remnants (thickness of the ZSZ has been exaggerated for presentation and not to scale), and **(e)** Bulk southwestward flow within the ZSZ during the E2 phase progressively reorienting a shear fabric MN to M3N3 and ultimately giving apparently top-NE shear sense in its present position. Overall bulk flow within the HHSZ has remained southwestward – directed. Not to scale.

beneath the ITSZ in the TMC to a maximum depth of about 100 km (Jain *et al.* 2003) and has undergone HP and UHP metamorphism around 55 Ma (Guillot *et al.* 1997, de Sigoyer *et al.* 2000, Mukherjee & Sachan 2001, Jain *et al.* 2003). The Tso Morari eclogites have suffered southwest verging intense ductile shearing and isoclinal folding before being rapidly exhumed during amphibolite and greenschist facies. These rocks have witnessed ubiquitously distributed extensional tectonics and doming during subsequent exhumation between 44 to 30 Ma, at least. Though no Cenozoic leucogranite bodies have been found so far within the TMC, it is likely that it represent 'cold' channel flow between 55-45 Ma after attaining UHP metamorphism.

As the Higher Himalayan Crystalline (HHC) slab is bound by low grade metasediments on either side, e.g. the Tethyan Sedimentary Zone in north and the Lesser Himalayan Sedimentary Zone in the south, it is evident that part of the HMB slab was broken off from the UHP Tso Morari Crystalline along the proto-HDS and being heated up and progressively regionally metamorphosed around 20–30 km depth as the HHC (Figs. 9a, b). As this belt undergoes sillimanite-K-feldspar or sillimanite-muscovite facies metamorphism, it causes migmatization leading to crustal anatexis and liberation of large quantities of fluid, which induced melting in a nearly-subhorizontal zone having maximum fluidity and tendency to flow. This melt remained trapped within the magma chamber due to confined overburden of the HHC metamorphics itself from 46 Ma until 20 Ma - a time span characterized by liberation of fluids and melts causing episodic growth of zircons, as is indicated by the SHRIMP-II U-Pb data. During this period, the granite remained trapped within migmatite zone in the core of the channel. Subsequently, this buyout melt was able to ascent through the crust from nearly middle of the channel in most cases during decompression, which is caused by exhumation of the channel through movements along the MCT in the lower parts and the extension in the upper sections. Granite bodies rose across the HHC slab and were emplaced in their current high-structural level along the extensional zone like the Zanskar/ Trans-Himadri Shear Zone around 20 Ma.

TECTONIC MODELS

Any 'realistic model' for tectonic evolution and its subsequent exhumation of the HMB should consider the following important observations:

i) **Tectonic boundaries:** MCT at the base with southwest-directed overthrusting and the HDZ with evidences both for overthrusting towards southwest and extension towards northeast.

ii) **Inverted metamorphism within the HHC**

a. ***Field disposition of metamorphic isograds:*** Inverted in lower parts of the slab, presence of migmatite and in situ granite in the middle or upper parts in association with highest-grade metamorphic sequences, and lower grade sequences in the upper parts.

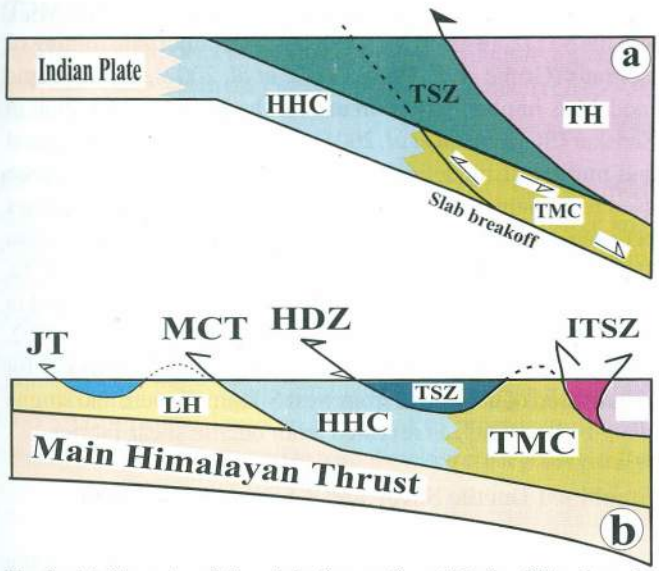

Fig. 9. **(a)** Geometry of the subducting continental Indian Plate along the ITSZ beneath tectonic units of the Trans-Himalaya (TH). The HHC and TMC have been shown in continuation with the Indian Plate and overlain by the Tethyan Sedimentary Zone (TSZ) cover before slab break of Arrows indicate possible movement sense of the Himalayan Metamorphic Belt (HMB), and **(b)** Present-day configuration of the Himalayan tectonic units due to continental collisionshowing merger of the MCT with the Main Himalayan Thrust (MHT) along which the Indian Plate is still subducting.

b. ***Relation with tectonic boundaries:*** Isograds truncated by the MCT at the base and the HDZ at the top; repeated and truncated within the HHC due to subsidiary thrusts like the Vaikrita/ Karcham Thrusts.

c. ***Regional dips:*** Uniformly dipping towards NE on regional scale, except for local large-scale folding in Zanskar and Beas Valley.

d. ***Thermobarometric data:*** Exhumation of the HHC from maximum temperature of 780°C and pressure of 10 Kb to 600°C and 4-6 Kb in Zanskar.

e. ***Textural constraints within the HHC and HDZ:*** Porphyroblastic growth both along S-and C-planes indicating syn – to late – tectonic growth and shear sense reversal.

iii) Shear sense: Continuous top-SW ductile shearing throughout the HHC including the HDZ during Eo-to Neo-Himalayan Period (16-25 Ma). Earlier top-SW sense of shear within the HDZ is superimposed by top-NE extensional shear sense.

iv) Simultaneity of the MCT and HDZ tectonic movements during Middle Miocene.

v) Recognition of ductile shearing as the most important exhumation mechanism.

vi) Zircon overgrowth in migmatite and leucogranite on older cores between 46 –20 Ma.

vii) Geophysical data indicating presence of fluid in middle crust in southern Tibet.

Ductile Shear Model

Proposed by Jain & Manickavasagam (1993) to explain the inverted metamorphism within the HHC of Zanskar, model looks at consistent top-SW sense of ductile shearing of the HHC along numerous discrete shear planes as a mechanism by which metamorphic isograds can be inverted within 15-20 km thick High Himalayan Shear Zone (HHSZ) (Fig. 5). Along with thermobarometric data, millimeters to decimeter scale displacement along each of such small shear zones have been calculated to exhume cumulatively the HHC metamorphics with displacements amounting to at least 80-120 km. Further work in other sections of the HHSZ by Manickavasagam *et al.* (1999) and Jain *et al.* (1999, 2002) have given more thermobarometric data in support of this model (also, Tripathi & Gairola 1999 for the Garhwal nappe). Consistent shear sense in the HHC right from its base (MCT) to the top (bottom of HDZ) as depicted in this model implies that 20 km thick HHC was considered as a single large shear zone with these tectonic boundaries as two walls. Unsheared lithounits within the HHC might be due to strain partitioning of the top-SW sense of shear. This top-SW sense of shear acting on the MCT and HDZ induced a consistent sense of shear within the HHC along numerous discrete shear planes in the same sense. Such a flow is completely controlled by relative shear movements of two walls. Simplifications in their model are: (i) brittle tectonics in HHC during the later part of exhumation was not considered, (ii) synorogenic extensional normal sense of shear within the HDZ, which superposes over the earlier thrust sense of shearing, was not taken into account. Thus, this model represents only the E1 exhumation in the HHC.

It is important to note that the term 'ductile shearing' incorporates both non-coaxial (simple shear) and coaxial deformations (pure shear), whereas Jain & Manickavasagam (1993) and Manickavasagam *et al.* (1999) have implied essentially non-coaxial deformation in using the term 'ductile shear model'. We retain the phrase 'ductile shear model' keeping in mind its stringent implication.

Channel Flow Model

Two end members of such flow are *flow induced by shear* (same as the ductile shear model already described) and the *plane Poiseuille flow* (Fig. 8c). Salient points of plane Poiseuille flow are as follows:

In this case, unidirectional flow of incompressible fluid takes place, through infinitely long mutually parallel and static channel walls devoid of any body force, due to constant pressure gradient (dP/dx). As per the choice of axes and flow direction in Fig. 8c, the flow is given by:

$$x = (\tfrac{1}{2}\mu)\ dP/dx\ (y_0^2 - y^2) \qquad \textbf{(Pai 1956)}$$

Mean velocity for such flow is two third of the maximum velocity, i.e.

$$V_{av} = -(1/2\mu)\ dP/dx\ y_o^2$$

Rate of mass flow across a station for such a flow is given by

$$M = -(2/3\mu)\ dP/dx\ y_o^3$$

At channel wall to fluid contact, the fluid velocity is zero; it increases across the channel parabolically, attains its maximum value $[-1/(2\mu)\ (dP/dx)\ y_0^2]$ at the center of the channel, and then decreases symmetrically and parabolically till it again attains zero value. The vorticity is zero at the vertex of the parabola and increases symmetrically across it and attains maximum values at the channel – fluid contacts. With a flow of this type, vertex flows with maximum velocity with subsequent thinning of parabola font. Sense of shear (or the sign of vorticity) will be opposite across middle of the channel. Geologically speaking, therefore, bulk unidirectional flow of this kind can give rise to *shear sense reversal (SSR)* across middle of the channel.

Two basic kinds of fluid flow are considered: plane couette and plane poiseuille flows in fluid mechanics (cf. Pai 1956). Out of these two, the second type, also referred to as 'channel flow' or 'pipe flow', has been used to approximately represent exhumation of shear zones. Channel flow model has become popular for shear zone exhumation (Daniel *et al.* 2003, Grujic *et al.* 2003, Searle & Szulc 2003), although Harrison & Yin (2003) have raised question on the validity of such rock flow. Experimental simulation of channel flow model in geological contexts is not yet available but Chemanda is carrying out this work (pers. comm.).

Plane Poiseuille flow model was, therefore, used for exhumation of the HHC in Bhutan as extrusion of a shallow crustal wedge along with top-SW and NE-shear of the MCT and the STDZ, respectively with post- metamorphic folding of isograds (Grujic *et al.* 1996, Grujic *et al.* 2002), and the same model has implicitly been in use for the HHSZ exhumation in Zanskar (Stephenson *et al.* 2001). Coupled thermal mechanical and numerical modeling of plane poiseuille flow have been used to explain ductile extrusion of high grade metamorphics between normal and thrust movements of the South Tibetan Detachment Zone (STDZ) and the Main Central Thrust (MCT), respectively in Nepal Himalaya (Beaumont *et al.* 2001), and in the Main Central Thrust Zone in general (Jamieson *et al.* 2002, 2004). Searle & Szulc (2003) have used channel flow model for exhumation of the HHSZ from west Sikkim for pure and simple shear components, as revealed from ductile shear fabrics.

Combined Ductile Shear and Channel Flow Model

Keeping various constraints of pure ductile shear and pure channel flow models and previously mentioned first order observations in mind, a combined ductile shear and channel flow model for deformation and exhumation in the NW Himalaya is presented. As earlier described in this paper, the whole process is divided into two stages: E = E1+ E2. The MCT and top of HDZ are considered as the walls of an orogenic channel. These models are mathematically defined in this work in terms of velocity profiles for laminar flow.

E1 Phase: We visualize that the HMB initially underwent UHP metamorphism during continental subduction ~55 Ma after the closure of the Tethyan Ocean along the ITSZ (Fig. 9a) and got exhumed southwestward as cold channel (Fig. 9b). But the main part of this slab of the HHC was subsequently broken from the HMB to undergo progressive regional metamorphism during Eo–Himalayan Period, possibly before 45 Ma. Main Himalayan D2 deformational phase caused intense crustal shortening within the HHSZ, bounded by the MCT at the base and the HDZ at the top and developed numerous top–SW ductile shear zones, which thrust it up with the same sense of shear. This part is modeled by 'idealized ductile shear model' (Jain & Manickavasagam 1993, Manickavasagam *et al.* 1999, Jain *et al.* 2002), or 'flow induced solely by simple shear'. It is postulated that metamorphic isograds within the Higher Himalaya were kinked making acute angle with the base of HDZ in top-SW direction and were subsequently modified in the next exhumation phase (Fig. 5). Although the term HDZ has been used in this phase, it didn't have a separate entity during E1. The model also postulates inversion of metamorphic isograds wherein highest like sillimanite-K-feldspar in Zanskar and sillimanite-muscovite in Beas-Bhagirathi Valleys are located in the upper parts. This phase also causes partial melting in these high grades, and generation of migmatite and in situ

leucogranite with episodic zircon overgrowth since 45 Ma till 20 Ma. This happens to be first record of initiation of flow of rock material 5 Ma in the Great Himalayan Channel (GHC), as has been termed here.

E2 Phase: (Figs. 10a-c) Viscosity of the HHC material was significantly reduced so that it acquired flow character and underwent fast exhumation by combined pressure gradient (plane Poiseuille Flow) and ongoing top-SW and shearing within the GHC (Fig. 10a). As the flow within the GHC enhanced through migmatization during decompressional exhumation since ~ 45 Ma episodically, migmatite zone also increased in thickness in deeper levels in mid crust to provide sufficient magmatic fluids to characterize partial molten crust geologically and geophysically (Fig. 10b). Granite melt remained trapped in interstitial pore spaces till 25Ma when it started migrating upwards through rock column as leucogranite dykes and sills at the base of the Tethyan sediments. This scenario is approximated by a combined 'ductile shear flow' and 'plane Poiseuille flow' and given by:

$$x = (U_X - U_Y)/2 + (U_X + U_Y)\, y/2\, y_0 - (\tfrac{1}{2}\mu)\, dP/dx\, (y_0^2 - y^2)$$

The vertex of this velocity profile is given by:

X ordinate:

$$(U_X - U_Y)/2 - (U_X + U_Y)^2/(8.y_0^2)\mu\, dx/dP - 1/(2\mu)\, dP/dx\, y_0^2$$

Y ordinate: $\mu_0(U_X + U_Y)/(2.y_0).dx/dP$

A line passing through vertex (V) and parallel to the MCT marks lower boundary of the HDZ. With progressive exhumation of this combined model type, V keeps on shifting parallel to channel wall upwards either across the GHS or obliquely to its strike. As is evident from the Zanskar P-data, pressure gradient is created by reduced pressure from 10 Kb during peak metamorphism to 4–6 Kb during exhumation and migmatization.

As the flow within the channel is enhanced episodically since ~45 Ma, migmatite zone also increases in thickness and in deeper levels in mid crust to provide sufficient magmatic fluids to characterize partial molten crust geologically and geophysically, as is evident in South Tibet (cf., Nelson *et al.* 1996). Granite melts remained trapped in interstitial pore spaces till 25–20 Ma when it started migrating upwards through pores as dykes and sills (Fig. 10c).

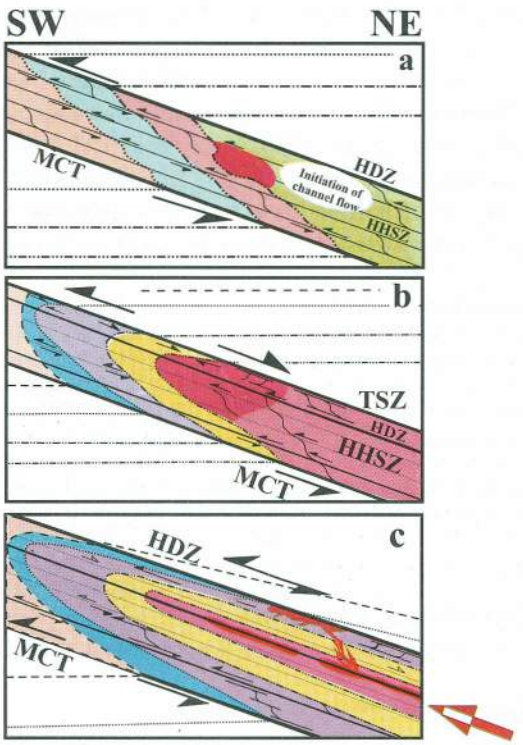

Fig. 10. Conceptual combined ductile shear and channel flow model for the Himalayan Metamorphic Belt (HMB) based on various data sets. **(a)** Initiation of flow in channel around 45 Ma from highest metamorphic isograds where migmatite and in situ leucogranite were generated. Other details are in Fig. 5. **(b)** Advancement of channel flow and reversal of channel-controlled shear indicators within the HDZ. Zone of highest isograds widens like in Zanskar, while the TSZ cover is also affected by high-grade metamorphism in Sutlej valley and **(c)** Combined ductile shear and channel flow model with narrow zone of migmatite and anataxis, e.g. Bhagirathi and Beas Valleys. Release of the Himalayan leucogranite ~ 25-20 Ma and their rise to the HDZ through dykes and sills and crystallization along extensional fault zone. Channel controlled shear fabric is shown by small open arrows.

CONCLUSIONS

New perspective thoughts on the Himalayan collision zone during the past decade and in recent years through concerted research efforts integrate geological, geochemical, geochronological and geophysical data in favor of evolution of the Himalayan Metamorphic Belt into a combined ductile shear zone and channel flow towards southwest since its episodic flow at least from 45 Ma. The Great Himalayan Channel has undergone initially top-SW ductile shearing, causing inverted metamorphism and migmatization during exhumation in the core of the channel. Zircon overgrowth from in situ leucogranite associated with migmatite ~45 Ma provide undisputed evidence for initiation of the channel flow in Eocene rather than Miocene, as has been currently

postulated. Viscous flow in the GHC widened progressively with time. Current signature of the presence of mid crustal fluids in southern Tibet and in southern parts of Karakoram and Trans-Himalaya are manifestations of growing and widening of magmatic fluids with geological time, whereas current exposures of migmatite and leucogranite in the Higher Himalaya are manifestation of tectonics rather than erosional-controlled exposures of the Great Himalayan Channel.

Acknowledgements: Various concepts in this work have emerged over the years through sustained research funded by the DST in which Dr. K. R. Gupta has played a very pivotal role in conceptualizing these programs and constant interaction. It is the tribute to Dr. Gupta's insight that such programs got various inputs including the HIMPROBE project of the DST that provided us an opportunity of investigate the most difficult parts of the Himalayan collision zone. Lot of concepts has emerged during the Invitation Fellowship to AKJ to Hokkaido University during summer 2004. SHRIMP analysis could only be possible through BOYSCOT Fellowship of the DST to SS who carried out analyses at university of Western Australia and Curtin University. Research on channel flow could only be made possible through the CSIR fellowship (FN 2-48/2001(II)EUII) to SM, who was also benefited by attending the 32nd IGC through 'Hutchison Young Scientist' Award by the Organizers.

References

Agarwal, N. C. & Kumar, G. 1973. Geology of the upper Bhagirathi and Yamuna Valleys, Uttarkashi district, Kumaun Himalaya. *Himalayan Geology*, **3,** 1-23.

Beaumont, C., Jamieson, R.A., Nguyen, M.H. & Lee, B. 2001. Himalayan tectonics explained by extrusion of a low-viscosity crustal channel coupled to focused surface denudation. *Nature*, **414,** 738-742.

Beaumont, C., Jamieson, R.A., Nguyen, M.H. & Medvedev S. 2004. Crustal Channel Flows: 1. Numerical models with application to the tectonics of the Himalayan-Tibetan Orogen. *Journal of Geophysical Research,* **109,** B06406, doi:10.1029/2003JB002809.

Brunel, M. 1986. Ductile thrusting in the Himalaya: shear sense criteria and stretching lineation. *Tectonics*, **5,** 247-265.

Burchfiel, B.C. & Royden, L.H. 1985. North-South extension within the convergent Himalayan region. *Geology*, **13**, 679-682.

Burchfiel, B.C., Chen, Zhiliang, Hodges, K.V., Liu Yuping, Royden, L.H., Changrong Deng & Xue, Jiene 1992. The South Tibetan detachment system, Himalayan orogen: Extension contemporaneous with and parallel to shortening in a collisional mountain belt. *Geological Society of America Special Paper,* **269,** 41p.

Coward, M.P., Jan, M.Q., Rex, D., Tarney, J., Thirlwall, M. & Windley, B. F. 1982. Geotectonic framework of the Himalaya of North Pakistan. *Journal of Geological Society London*, **139**, 299-308.

Davidson, C., Grujic, D.E., Hollister, L.S. & Schmid, S.M. 1997. Metamorphic reactions related to decompression and synkinematic intrusion of leucogranite, High Himalayan Crystallines, Bhutan. *Journal of Metamorphic Geology*, **15,** 563-612.

Daniel, C.G., Hollister, L.S., Parrish, R.R. & Grujic, D. 2003. Exhumation of the Main Central Thrust from lower Crustal Depths, Eastern Bhutan Himalaya. *Journal of Metamorphic Geology*, **21**, 317- 334.

de Sigoyer J., Chavagnac V., Blichert-Toft J., Villa I., Luais B., Guillot S., Mascle G. & Cosca M. 2000. Dating continental subduction and collisional thickening in NW Himalaya: Multichronometry of the Tso Morari eclogites. *Geology*, **28**(6), 487-490.

Dèzes, P.J, Vannay, J.C., Steck, A., Bussy, F. & Cosca, M. 1999. Synorogenic extension: Quantitative constraints on the age and displacement of the Zanskar shear Zone. *Geological Society of America Bulletin*, **111**, 364-374.

Edwards, M.A. & Harrison, T.M. 1997. When did the roof collapse? Late Miocene N-S extension in the High Himalaya revealed by Th-Pb monazite dating of Khula-Kangri granite. *Geology*, **25,** 543-546.

Epard, J. -L., Steck, A., Vannay, J. -C. & Hunziker, J. 1995. Tertiary Himalayan structures and metamorphism in the Kulu Valley (Mandi-Koksar transect of the western Himalaya) - Shikar Beh Nappe and crystalline Nappe. *Schweizerische Mineralogische und Petrographische Mitteilungen*, **75,** 59-84.

Ferrara, G., Lombardo, B. & Tonarinia, S. 1991. Sr, Nd and O isotopic characterization of the Gumburanjan leucogranites (High Himalaya). *Schweizerische Mineralogische und Petrographische Mitteilungen*, **71,** 35-51.

Foster, G., Kinny, P., Vance, D., Prince, C. & Harris, N. 2000. The significance of monazite U-Th-Pb age data in metamorphic assemblages; a combined study of monazite and garnet chronometry. *Earth and Planetary Science Letters*, **181,** 327-340.

Frank, W., Hoiekes, G., Miller, C., Purtscheller, F. Richter, W. & Thoni, M. 1973. Relations between metamorphism and orogeny in a typical section of the Indian Himalayas. *Tschermaks Mineralogische Und Petrographische Mitteilungen*, **20,** 303-332.

Frank, W., Thoni, M & Purtscheller, F. 1977. Geology and petrography of Kulu-South Lahul area. *In : Ecologie et geologie de l'Himalaya*, Paris, Dec. 7-10, **33,** 147-172.

Gansser, A. 1964. *Geology of the Himalayas*, Wiley-Interscience, London. 289p.

Girard, M. & Bussy, F. 1999. Late Pan-African magmatism in Himalaya: new geochronological and geochemical data from the Ordovician Tso Morari metagranites (Ladakh, NW India). *Schweizerische Mineralogische und Petrographische Mitteilungen*, **79,** 399-418.

Godin, L., Brown, R.L. & Hanmer, S. 1999. High strain zone in the hanging wall of the Annapurna detachment, central Nepal Himalaya. *In*: Macfarlane, A., Sorkhabi, R.B. & Quade, J. *(eds.), Himalaya and Tibet: Mountain Roots to Mountain Tops*. Geological Society of America, Special Paper, **328,** 199-210.

Grujic, D., Casey, M., Davidson, C., Hollister, L.S., Kündig, R., Pavlis, T. & Schmid, S., 1996. Ductile extrusion of the Higher Himalayan Crystalline in Bhutan: evidence from quartz microfabrics. *Tectonophysics*, **260**, 21-43.

Grujic, D., Hollister, L.S. & Parrish, R.R. 2002. Himalayan metamorphic sequence as an orogenic channel: insight from Bhutan. *Earth and Planetary Science Letters*, **198**, 177-191.

Gulliot, S., de Sigoyer, J., Lardeaux, J. M., Mascle, G. & Colchen, M. 1997. Eclogitic metasediments from the Tso Morari area (Ladakh Himalaya): Evidence for continental subduction during India-Asia convergence. *Contibution to Mineralogy and Petrology*, **128,** 197-212.

Gulliot, S., Cosca, M., Allemand, P. & Le Fort, P. 1999. Contrasting metamorphic and geochronologic evolution along the Himalayan belt. *In*: Macfarlane, A., Sorkhabi, R. B. & Quade, J. *(eds.) Himalaya and Tibet: Mountain Roots to Mountain Tops*. Geological Society of America, Special Paper, **328,** 117-128.

Harrison, T.M., Grove, M, Lovera, O.M., Catlos, E.J. & D'Andrea, J. 1999. The origin of Himalayan anatexis and inverted metamorphism: Models and constraints. *Journal of Asian Earth Sciences*, **17**, 755-772.

Harrison, T. M., Ryerson, F. J., Le Fort, P., Yin, A., Lovera, O. & Catlos, E. J. 1997. A late Miocene-Pliocene origin for the central Himalayan inverted metamorphism: *Earth and Planetary Science Letters*, **146,** E1-E7.

Harrison, T. M. & Yin, A. 2002. Did the Himalaya extrude from beneath the Tibetan plateau? *Abstract Volume. 18th Himalaya-Karakoram-Tibet Workshop*. Monte Verita. 57-58.

Herren, E. 1987. Zanskar Shear Zone: northeast-southwest extension within the Higher Himalaya (Ladakh, India). *Geology*, **15,** 409-413.

Hodges, K.V. 2000. Tectonics of the Himalaya and southern Tibet from two perspectives. *Geological Society of America Bulletin*, **112**(3), 324-350.

Hodges, K.V. & Silverberg, D.S. 1988. Thermal evolution of the greater Himalaya, Garhwal, India. *Tectonics*, **7,** 583-600.

Hubbard, M. 1989. Thermobarometric constraints on the thermal history of the Main Central thrust zone and Tibetan slab, eastern Nepal Himalaya. *Journal of Metamorphic Geology*, **7,** 19-30.

Jain, A.K. & Anand, A. 1988. Deformational and strain patterns of an intracontinental collision ductile shear zone an example from the Higher Garhwal Himalaya. *Journal of Structural Geology*, **7,** 717-734.

Jain, A.K. & Manickavasagam, R.M. 1993. Inverted metamorphism in the intracontinental ductile shear zone during Himalayan collision tectonics. *Geology*, **21,** 407-410.

Jain, A.K. & Manickavasagam, R.M. 1997. Ductile shear as a cause of inverted metamorphism: Example from the Nepal Himalaya: A discussion. *Journal of Geology*. **105,** 511-514.

Jain, A.K. & Patel, R.C. 1999. Structure of the Higher Himalayan crystalline along the Suru-Doda valleys (Zanskar), NW Himalaya. *In*: Jain, A. K. Manickavasagam, R.M. (eds.), *Geodynamics of the NW Himalaya*. Gondwana Research Group Memoir, **6,** 91-110.

Jain, A.K., Manickavasagam, R.M. & Singh, Sandeep 1999. Collision tectonics in the NW Himalaya: deformation, metamorphism, emplacement of leucogranite along Beas-Parbati Valleys, Himachal Pradesh. *In*: Jain, A. K. & Manickavasagam, R. M. (eds.), *Geodynamics of the NW Himalaya*. Gondwana Research Group Memoir, **6,** 3-37.

Jain, A.K., Singh, Sandeep & Manickavasagam, R.M. 2002. *Himalayan Collision Tectonics*. Gondwana Research Group Memoir, **7,** 114 p.

Jain, A. K., Singh, S., Manickavasagam, R. M., Joshi, M. & Verma, P. K. 2003. HIMPROBE Programme: integrated Studies on Geology, Petrology, Geochronology and Geophysics of the Trans-Himalaya and Karakoram. *Memoir of Geological Society of India*, **53,** 1-56.

Jamieson, R. A., Beaumont, C., Nguyen, M. H. & Lee, B. 2002. Interaction of metamorphism, deformation and exhumation in large convergent orogens. *Journal of Metamorphic Geology*, **20,** 9-24.

Jamieson, R. A., Beaumont, C., Medvedev, S. & Nguyen, M. H. 2004. Crustal Channel Flows: 2. Numerical models with implications for metamorphism in the Himalayan-Tibetan Orogen. *Journal of Geophysical Research,* **109**, B06407, doi:10.1029/2003JB002811.

Le Fort, P. 1975. Himalayas: The collided range, Present knowledge of the continental arc. *American Journal of Science,* **275,** 1-44.

Leech, M E., Singh, S., Jain, A. K. & Manickavasagam, R. M. 2003. New U-Pb SHRIMP ages for the UHP Tso-Morari Crystallines, Eastern Ladakh, India. *The Geological Society of America (GSA) Annual Meeting, Seattle, USA*, Abstract no. 61682, Paper No. 260-24

Manickavasagam, R. M., Jain, A. K., Singh, Sandeep & Asokan, A. 1999. Metamorphic evolution of the NW-Himalaya, India: Pressure-temperature data, inverted metamorphism, and exhumation in the Kashmir, Himachal, and Garhwal Himalaya. *In*: Macfarlane, A., Sorkhabi, R. B. & Quade, J. (eds.), *Himalaya and Tibet: Mountain Roots to Mountain Tops*. Geological Society of America Special Paper, **328** 179-198.

Mattauer, M. 1986. Intracontinental subduction, crust-mantle decollement and crustal-stacking wedge in the Himalaya and other collision belts. *In*: Coward, M. P. & Ries, A. (eds.) *Collision Tectonics*. Special Publication, Geological Society London No.**10,** 37-50.

Metcalfe, R.P. 1993. Pressure, temperature and time constraints on metamorphism across the Main Central thrust zone and High Himalayan slab in the Garhwal Himalaya. *In*: Treloar, P. J. & Searle, M. P. (eds.), *Himalayan Tectonics*. Special Publication, Geological Society London, **74** 485-509.

Mukherjee, B. K., & Sachan, H. K. 2001. Discovery of coesite from Indian Himalaya: A record of ultra-high pressure metamorphism in Indian Continental Crust. *Current Science*, **81**(10), 1358-1361.

Nelsen, K. D., Zhao, W. & INDEPTH Project Team 1996. Partially molten middle crust beneath southern Tibet: Synthesis of Project INDEPTH Results. *Science*, **274,** 1684-1688.

Noble, S. R. & Searle, M. P. 1995. Age of crustal melting and leucogranite formation from U-Pb zircon and monazite dating in the Western Himalaya, Zanskar, India. *Geology*, **23**(12), 1135-1138.

O'Brien, P.J., Zotov, N., Law, R., Khan, M.A. & Jan, M.Q. 2001. Coesite in Himalayan eclogite and implications for models of India-Asia collision. *Geology*, **29,** 435-438.

Pai, S. -I. 1956. *Viscous Flow Theory I- Laminar Flow.* D. Van Nostrand Company Inc. New Jersey.

Patel, R. C., Singh, Sandeep, Asokan, A., Manickavasagam, R. M. & Jain, A. K. 1993. Extensional tectonics in the collisional Zanskar Himalayan belt *In*: Treloar, P. J. & Searle, M. P. (eds.), *Himalayan Tectonics*. Special Publication, Geological Society London, **74** 445-459.

Pecher, A., Bouchez, J-L. & Le Fort, P. 1991. Miocene dextral shearing between Himalaya and Tibet. *Geology*, **19**, 683-685.

Pognante, U. & Lambardo, B. 1989. Metamorphic evolution of the Higher Himalayan crystalline in SE Kashmir, India. *Journal of Metamorphic Geology*, **7** 9-17.

Pognante, U., Castelli, D., Benna, P., Genovese, G., Obreli, F., Meier, M. & Tonarini, S. 1990. The crystalline units of the High Himalayas in the Lahul-Zanskar region (northwest India) metamorphic-tectonic history and geochronology of the collided and imbricated Indian plate. *Geological Magzine*, **127,** 101-116.

Prince, C. I., Kosler, J., Vance, D. & Gunther, D. 2000. Comparison of Laser ablation ICP-MS and isotope dilution REE analyses – implications for Sm-Nd garnet geochronology. *Chemical Geology*, **168,** 255-274.

Searle, M. P.& Godin, L. 2003. The South Tibetan Detachment and the Manaslu Leucogranite: a Structural Reinterpretation and Restoration of the Annapurna-Manaslu Himalaya, Nepal. *Journal of Geology,* **111** 505-523.

Searle, M. P. & Szulc, A. G. 2003. Channel flow and ductile extrusion of the High Himalayan slab- the Kangchenjunga-Darjeeling profile, Sikkim Himalaya. *18th Himalaya-Karakoram-Tibet Workshop, Monte Verita, Abstract Volume,* 108-109.

Searle, M.P., Simpson, R.L., Law, R.D., Parrish, R.R. & Waters, D.J. 2003. The structural geometry, metamorphic and magmatic evolution of the Everest massif, High Himalaya of Nepal-South Tibet. *Journal of the Geological Society, London,* **160,** 345-366.

Sharma V. P. 1977. The stratigraphy and structure of parts of the Simla Himalaya. *Memoir of Geological Survey of India*, **106,** 488p.

Srikantia, S.V. & Bhargava, O.N. 1998. *Geology of Himachal Pradesh.* Geological Society of India, 416p.

Stephenson, B.J., Waters, D. J. & Searle, M. P. 2000. Inverted metamorphism and the Main Central thrust: field relations and thermobarometric constraints from the Kishtwar Window, NW Indian Himalaya. *Journal of Metamorphic Geology*, **18,** 571-590.

Stephenson, B. J., Searle, M. P., Waters, D. J. & Rex, D. C. 2001. Structure of the Main Central Thrust zone and extrusion of the High Himalayan deep crustal wedge, Kishtwar-Zanskar Himalaya. *Journal of the Geological Society, London*, **158,** 637-652.

Thakur, V. C. 1993. *Geology of the Western Himalaya*. Pergmon Press, Oxford and New York, 355p.

Treloar, P. J., Broughton, R. D., Williams, M. P., Coward, M. P. & Windley, B. F. 1989. Deformation, metamorphism, and imbrication of Indian plate, south of the Main mantle thrust, north Pakistan. *Journal of Metamorphic Geology*, **7,** 111-126.

Tripathi, A. & Gairola, V.K. 1999. P-T conditions of metamorphism in the Garhwal Nappe. *In*: Jain, A. K. & Manickavasagam, R. M. (eds.), *Geodynamics of the NW Himalaya*. Gondwana Research Group Memoir **6**, 167-172.

Valdiya, K. S. 1980. *Geology of the Kumuan Lesser Himalaya*. Dehra Dun, Wadia Institute of Himalayan Geology, 291p.

Valdiya, K. S. 1987. Trans-Himadri fault and domal upwarps immediately south of the collision zone. *Current Science,* **56,** 200-209.

Valdiya, K. S. 1989. Trans-Himadri intracrustal fault and basement upwarps south of Indus-Tsangpo Suture Zone. *In*: Malinconico, L. L. & Lillie, R. J. (eds.), *Tectonics of the western Himalaya.* Geological Society of America Special Paper, **232** 153-168.

Vance, D. & Harris, N.B.W. 1999. Timing of prograde metamorphism in the Zanskar Himalaya. *Geology*, **27**, 395-398.

Vannay, J.C. & Grasemann, B. 1998. Inverted metamorphism in the High Himalaya of Himachal Pradesh (NW India): Phase equilibria versus thermobarometry. *Schweizerische Mineralogische und Petrographische Mitteitungen* **78**, 107-132.

Vannay, J.C. & Hodges, K.V. 1996. Tectonometamorphic evolution of the Himalayan metamorphic core between Annapurna and Dhaulagiri, central Nepal. *Journal of Metamorphic Geology*, **14,** 635-656.

Vannay, J.C., Sharp, D.Z. & Grasemann, B. 1999. Himalayan inverted metamorphism constrained by oxygen thermometry. *Contribution to Minerology and Petrology*, **137,** 90-101.

Walker, J.D., Martin, M.W., Bowring, S.A., Searle, M.P., Waters, D. J. & Hodges, K.V. 1999. Metamorphism, melting and extension: age constraints from the High Himalayan slab of southeast Zanskar and northwest Lahul. *Journal of Geology*, **107**, 473-495.